COMPUTATIONAL MODELING OF PATHWAY DYNAMICS FOR DETECTING DRUG EFFECTS: PARADOXICAL EFFECTS OF LY303511 ON TRAIL-INDUCED APOPTOSIS

Yuan Shi[1], Simi M. Varghese[2], Sinong Huang[3], Jacob White[1,4], Shazib Pervaiz[*,1,3,5,6], Lisa Tucker-Kellogg[*,1,2]

[1] Singapore-MIT Alliance, E4-04-10, 4 Engineering Drive 3, Singapore 117576, [2] Department of Computer Science, National University of Singapore, Singapore 117417, [3] Department of Physiology, NUS, 2 Medical Drive, Singapore 117597, [4] Department of Electrical Engineering and Computer Science, M.I.T., Cambridge, MA, USA 02139, [5] NUS Graduate School for Integrative Sciences and Engineering, Singapore, [6] Duke-NUS Graduate Medical School, National University of Singapore 117597.

** Correspondence to Lisa Tucker-Kellogg [tucker@comp.nus.edu.sg] or Shazib Pervaiz [phssp@nus.edu.sg]*

Based on previous work showing that the drug LY303511 sensitizes cancer cell lines to TRAIL-induced apoptosis, we used computational modeling and ordinary differential equations to represent how each agent individually affects the system. We then simulated the combined effects of both agents together, and found that the level of death *in silico* correlated well with experimental observations, including the synergistic (greater than additive) level of death from the combination treatment. However, simulation and experimental data exhibited numerous mismatches for some molecules upstream in the pathway, at time points shortly after treatment, such as differences in the slope and onset of the synergistic activation of caspase-8. Additional measurements of caspase-8 revealed a paradoxical caspase-inhibitory effect of LY303511 at early time points after treatment. This recent finding is seemingly at odds with the long-term effects of LY303511 towards promoting cell death. Moreover, LY303511 treatment was found to cause up-regulation of the protein cFLIP-s within one hour, followed by a decrease relative to untreated. Because cFLIP-s has often been found to antagonize caspase-8 activation, our cFLIP-s results suggest a possible explanation for the early caspase-inhibitory effect of LY303511. Further work remains, but the mathematical modeling approach used here may be of general use for identifying unknown effects of any drug (or perturbation), provided the drug is acting on a well-understood molecular pathway.

1. INTRODUCTION

Combinations of drugs can have non-obvious effects on a biological system, and the magnitude of their final effect can be synergistic, additive or antagonistic; meaning larger, the same as, or smaller than the sum of the individual treatments[1]. For treating cancers, some of the current standards of care are combination therapies, but the development of synergistic combinations has been an expensive and laborious process of empirical testing[2]. Computational modeling of pathway dynamics has the potential to predict the effects of combination treatments, and could be useful in the design of multi-drug therapies. Single perturbations of a system (e.g., inhibiting an enzyme) are commonly studied using traditional experimental methods, but combinations of perturbations, too numerous to study experimentally, could easily be examined exhaustively using computational tools. Additional applications of predictive models might also include designing modifications to metabolic networks for biomanufacturing[3]. We used modeling to study the combination of TRAIL and LY303511, towards understanding their synergy, and also aiding in the discovery of an unknown effect of LY303511.

The polypeptide ligand TRAIL (TNF-Related Apoptosis-Inducing Ligand or Apo2L) induces death receptor-mediated apoptosis (programmed cell death) according to a well-studied pathway. TRAIL is currently undergoing phase I/II clinical evaluation for a variety of cancers[4], and it holds real promise as a therapeutic strategy due to its selective targeting of cancer cells while sparing normal tissues[5]. However, development of resistance is a serious obstacle to the effective clinical use of TRAIL[6], and combination therapies to overcome resistance to TRAIL, or to induce re-sensitization to TRAIL, could be extremely important for enabling TRAIL-based therapies to succeed[6-9].

The small molecule compound LY303511 ("LY30") has been shown to sensitize multiple cancer cell lines to TRAIL-induced apoptosis[10,11] and vincristine-induced apoptosis[10]. LY30 is an inactive analogue of the PI3K inhibitor LY294002, and it is related to the non-specific kinase inhibitor quercetin[8,12-15]. Poh *et al.* and Shenoy *et al.* found a synergistic effect by combining LY30 and TRAIL. Namely, treating cells with low doses of TRAIL together with low doses of LY30 caused robust activation of the apoptotic pathway, while treatment with either of the agents alone caused minimal activation. Mediators of the LY30-induced sensitization to apoptosis have been reported and further investigation is ongoing.

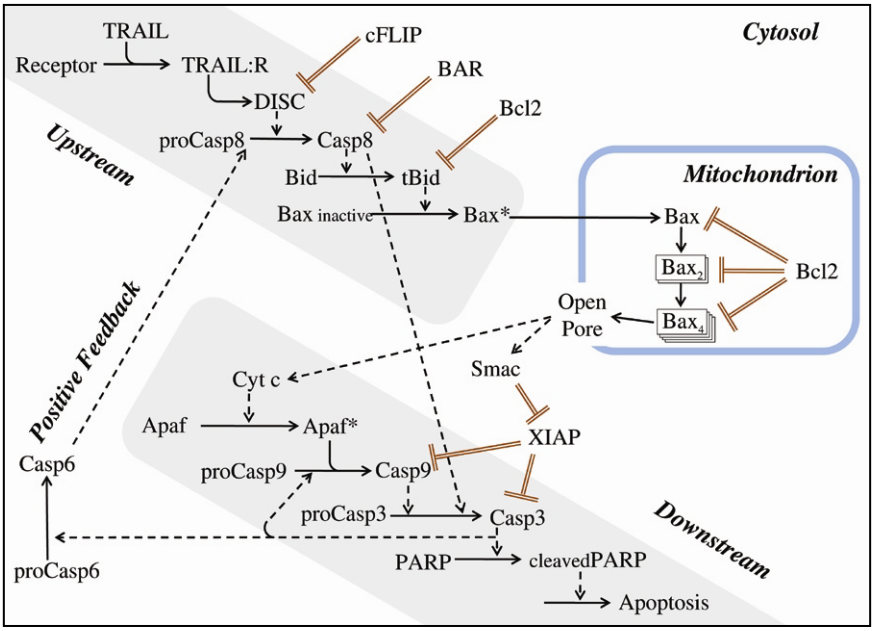

Fig.1. Schematic diagram of TRAIL-induced apoptosis. The dashed arrows indicate that the species at the base of the arrow is not consumed in the reaction (e.g., catalysis). Solid arrows indicate that the species at the base is consumed or translocated. For example, the oligomerization of mitochondrial Bax leads to formation of a pore in the mitochondrial outer membrane, which allows release of cytochrome c and Smac into the cytosol. Double-lines in a T indicate inhibitory effects, with the details of inhibition (binding, degradation, etc.) confined to Appendix A for simplicity of display. Synthesis and degradation are also not shown.

We undertook the task of modeling the effects of LY30 in the network of TRAIL-induced apoptosis, with the aim of evaluating whether the molecular effects known to be caused by LY30 were sufficient to explain the synergy of the LY30-TRAIL combination. We were successful at using modeling to recapitulate the synergistic levels of cell death that were observed. However, the simulated activation kinetics of pro-apoptotic caspase enzymes along the pathway showed poor correlation with experimental data. In particular, there were large mismatches between simulation and experiment at early time points, particularly for upstream regions of the pathway. This suggested further experiments focusing on caspase-8 activation shortly after treatment. This new data revealed an even larger and more obvious mismatch between simulation and experimental data. Specifically, LY30 treatment had a mild inhibitory effect on caspase-8, very soon after treatment. Finally we set out to investigate the upstream events responsible for the early inhibitory effect of LY30 on caspase-8 activation.

Although this paradoxical caspase inhibitory effect is eventually dwarfed by later apoptosis-promoting activity, the phenomenon raises new issues that should be investigated further, if LY30 is to be considered for clinical use. Computational modeling served as a magnifying glass for careful interpretation of experimental data and for detecting a subtle divergence between theory and observation. Modeling suggested a direction for experimental work that uncovered a novel effect. Our approach could be of general use for finding unknown effects of any drug or other agent, in the context of a well-understood signaling network.

2. METHODOLOGY AND RESULTS

2.1. TRAIL model

To study the synergy between LY30 and TRAIL, we adapted the model of TRAIL-induced apoptosis by Albeck *et al*., [16,17] and we added reaction equations for the impact of LY30 on the network. All biological reactions in the Albeck model are segmented into elementary reactions such as A + B → C. Interactions involving enzymes or multimolecular complexes are broken into a series of bimolecular reactions. The Albeck model of TRAIL-induced apoptosis is supported by extensive experimental measurements in HeLa cervical carcinoma cells. A primary focus of their model

is in recapitulating the phenomenon of "mitochondrial amplification," whereby significant but not lethal levels of activated caspase-8 can trigger permeabilization of the mitochondrial outer membrane and sudden release of apoptotic factors into the cytosol. The experiments by Albeck *et al*. for modeling and calibrating TRAIL-induced apoptosis were performed with cycloheximide, an inhibitor of protein synthesis. Because their model lacks explicit synthesis and degradation, even the slightest pro-apoptotic input is able to accumulate unrealistically, without degradation, until the cell eventually dies[18,19]. For this reason, we included complex biological influences, such as synthesis and degradation, by approximating them with simple mass-action rate equations (Appendix A and Supplementary Tables). This modification renders the model qualitative rather than quantitative, useful for inferring general trends and not for predicting absolute concentrations. We made two additional modifications of the Albeck model, adding a feedback loop from activated caspase-3 to active/activated caspase-9[20], and changing the parameters for the protein cFLIP (cellular FADD-like interleukin-1β-converting enzyme inhibitory protein) because it is particularly sensitive to cycloheximide[21]. Our modified model contains 67 species with 21 non-zero initial concentrations, 67 reactions, and 95 rate constants (Fig.1). Rate constants for protein synthesis and degradation are constrained by previous literature plus requiring the initial concentrations to equal the steady state. All other concentrations and rate constants are duplicated from the Albeck model unless otherwise indicated.

2.2. LY30 model

Starting with the model of TRAIL-induced apoptosis from section 2.1, we added reactions for LY30 as shown in Figure 2. Two effects of LY30 found by Poh *et al.* would likely contribute to the ability of LY30 to sensitize cells to TRAIL: (a) clustering of TRAIL receptors, and (b) down-regulation of the pro-survival protein cFLIP[22]. Clustering or oligomerization is modeled by an LY30-catalyzed transition in the TRAIL receptor, converting a slow-reacting unclustered form into a faster-reacting form that we designate clustered, in reference to the cross-linking experiments of Poh *et al.* that show a non-activating association between receptors. The cFLIP down-regulation is modeled as an LY30-catalyzed degradation reaction, which is intended to represent a variety of possible mechanisms including transcriptional repression, ubiquitylation, etc. In addition, LY30 had previously been shown to elevate intracellular hydrogen peroxide (H_2O_2)[10], which can promote death in a variety of ways[23-28]. Here we model H_2O_2 as causing low levels of caspase-9 activation[27,28], and also causing a small amount of death independent of this apoptotic pathway. Our model is restricted to TRAIL-induced apoptosis in HeLa cells, and we exclude data from other cell types[11] and other mechanisms of death signaling[14], unless stated otherwise. Our computational models are specified fully in the supplement at www.comp.nus.edu.sg/~tucker/ LY30-Supplement.pdf.

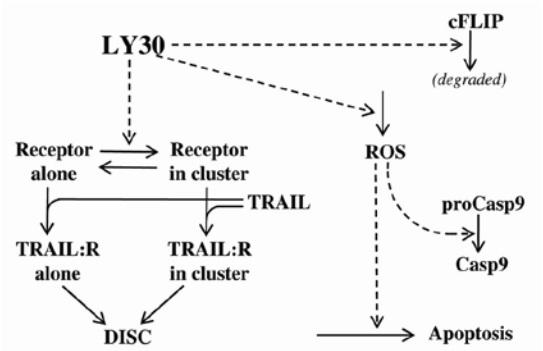

Fig.2. Schematic diagram of the modeled effects of LY30 on the pathway of TRAIL-induced apoptosis. The receptor alone or TRAIL:R alone would be expected to have slower rate coefficients than the same proteins in a clustered environment. Parameter values are listed in the supplement.

2.3. LY30+TRAIL model

This model is a combination of the two models explained above, with no other modifications. The simulation of a combination treatment follows the experimental protocol of Poh *et al.* preincubating cells with LY30 for one hour before treating with TRAIL. Converting this to the model means the initial concentration of TRAIL is zero initially, and then set to its non-zero initial concentration after 60 minutes of simulated preincubation.

3. MODELING SYNERGY

Extensive measurements of apoptotic signaling in HeLa cells after treatment with LY30 were published by Poh *et al.*; LY30 plus TRAIL were found to induce synergistic (greater than additive) activation levels at many stages of the apoptotic pathway, including strong, synergistic activation of initiator and executioner

caspases. To reduce the impact of measurement noise in assessing the synergy of this system, we performed additional replications of the cell viability measurements using the same methods, reagents, and strain of cells. The pooled dataset (Fig. 3) shows cell death to occur synergistically, with the rate of killing 30% higher than the rate expected from a purely additive effect.

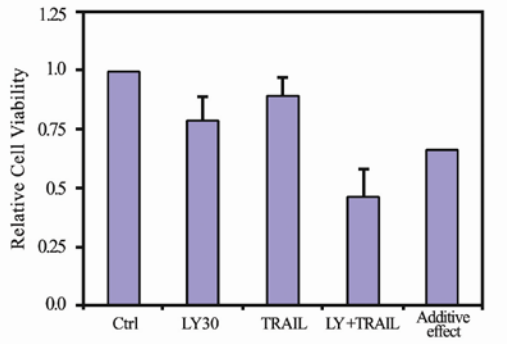

Fig.3. Relative cell viability (crystal violet assay at 18 hrs) after treatment with LY30 and/or TRAIL. The bar showing a hypothetical "additive effect" was computed by summing the average cell death levels for LY30 alone and TRAIL alone.

As shown previously[17,29], single cells undergo apoptosis as a "snap action" switch, preceded by a variable time delay. This causes single cells to exhibit sharp slopes in their activation levels, although a population of supposedly homogeneous cells exhibit a gradual slope. Because our model will be compared with immunoblots and enzyme activity assays performed on populations of cells, we need to model a population as well. We used Monte Carlo sampling to compute an average trajectory, using simulations of 10,000 instances for each treatment condition, and using normally distributed initial concentrations with 40% variance. An illustration of the averaging concept is shown in Figure 4a (with fewer than 10,000 samples for ease of display). Figure 4b compares the simulated viability of a single cell against the experimental viability for the treatment combinations. Our simulations were successful at recapitulating the experimentally observed synergy. This finding provides a "proof of plausibility" that death receptor clustering, cFLIP down-regulation, and H_2O_2 production are sufficient to facilitate significant sensitization, in cells treated with otherwise sub lethal doses of TRAIL.

4. MISMATCH OF THE MODEL

When we inspected the temporal profiles of proteins along the apoptotic pathway, we found the simulations did not resemble the experimental data. Note that the experimental measurements are quantified as fold-changes relative to control, and the data is compared to the model by its qualitative trends and curve-shape rather than by absolute concentration levels. Monte Carlo simulations predict that the synergistic activation of caspases by LY30 and TRAIL would begin quickly and increase steeply, relative to the rate at which the caspases are activated by LY30 alone or TRAIL alone. In contrast, experiments show synergistic activation occurring later, with no synergy at early time points. Enzymatic activity of caspase-8 shows no synergy between LY30 and TRAIL at 3hr or 6hr (Fig.5a). A milder version of the same mismatch is seen in caspase-3 at 3hr and 6hr (Fig. 5b).

Multiple efforts at parameter estimation[30-34] were unable to rectify the qualitative divergence between the model and the data. Supplementary figures, showing simulations of the model after random parameter perturbations of 10%, suggest that early synergy is a common outcome of the model, and that abolishing early synergy tends to abolish late synergy as well. Because our model optimization procedures were guided by sparse and noisy data, we sought to collect additional data to reduce the uncertainty of the search. Meanwhile we also hypothesized that unknown early phenomena in the cellular response to LY30 and TRAIL might be impossible to capture using the current network of reactions. Both of these considerations led us to investigate upstream proteins at early time points.

5. EXPERIMENTAL MEASUREMENTS

The mismatch observed in the simulations provided a relatively narrow specification for the molecules and time points in greater need of clarification. New experiments were performed to measure caspase-8 activity after treatment with LY30 and/or TRAIL (Fig. 6a), with additional early time points. Surprisingly, at early time points, LY30-treated cells showed less caspase-8 activity than untreated control cells. These experimental data points are in disagreement with our model of LY30 having purely pro-apoptotic effects.

We pursued the solo effects of LY30 in further experiments. Figure 6b shows the effect of LY30 on caspase-8 activity over time. To achieve better signal to noise ratio, current experiments were pooled with previously published data[35] (using the same reagents, methods, and strain of cells). The caspase-8 activation

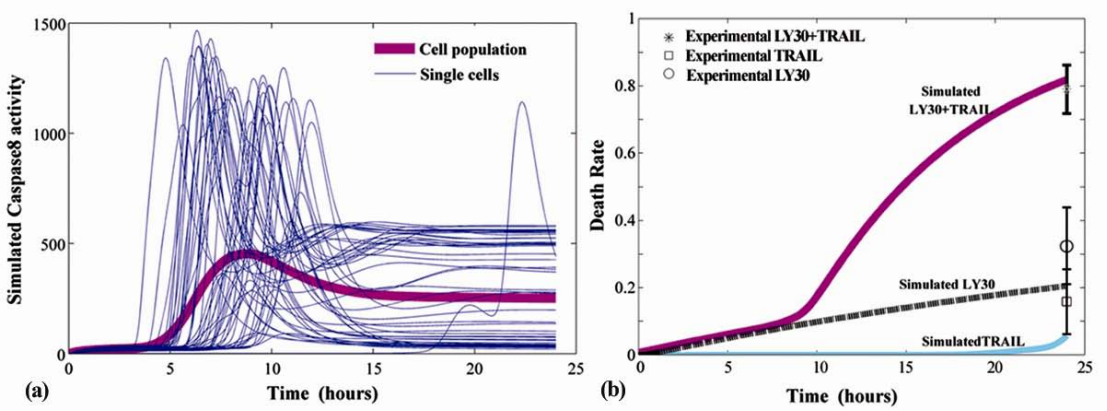

Fig. 4. Simulations using Monte Carlo sampling. (a) An example of the method showing the effect of averaging. (b) Comparison of relative cell viability by simulation and experiment.

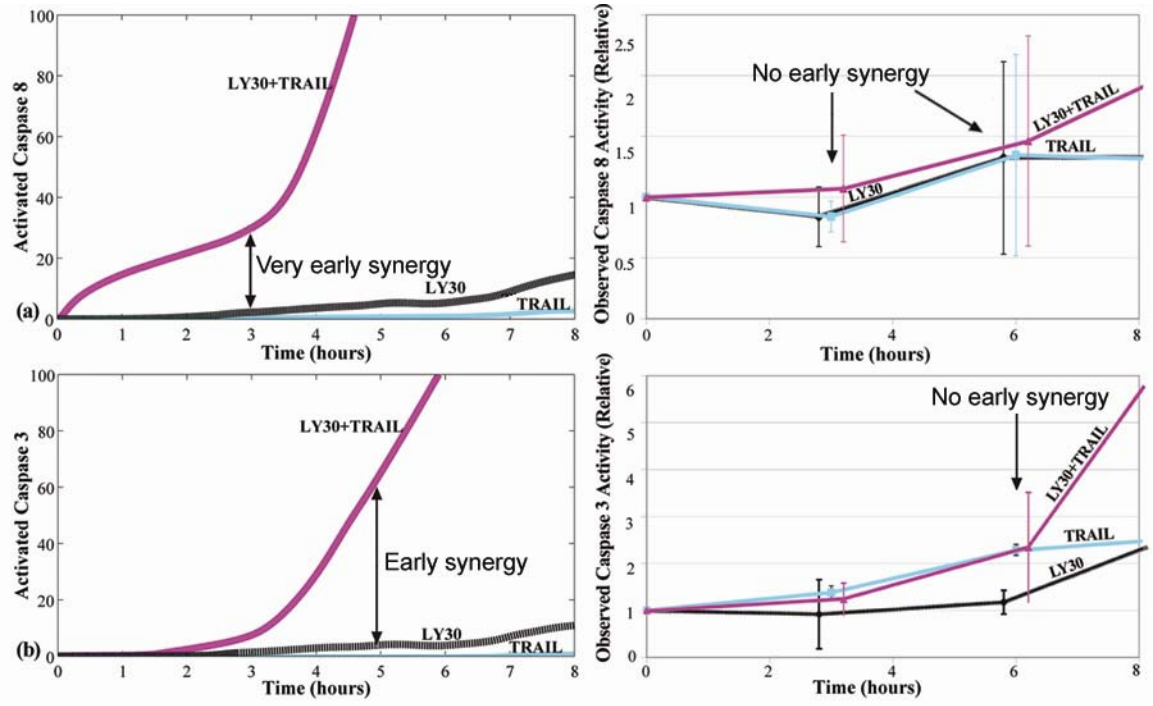

Fig. 5. Deviation of caspase activity between the model and experiments.

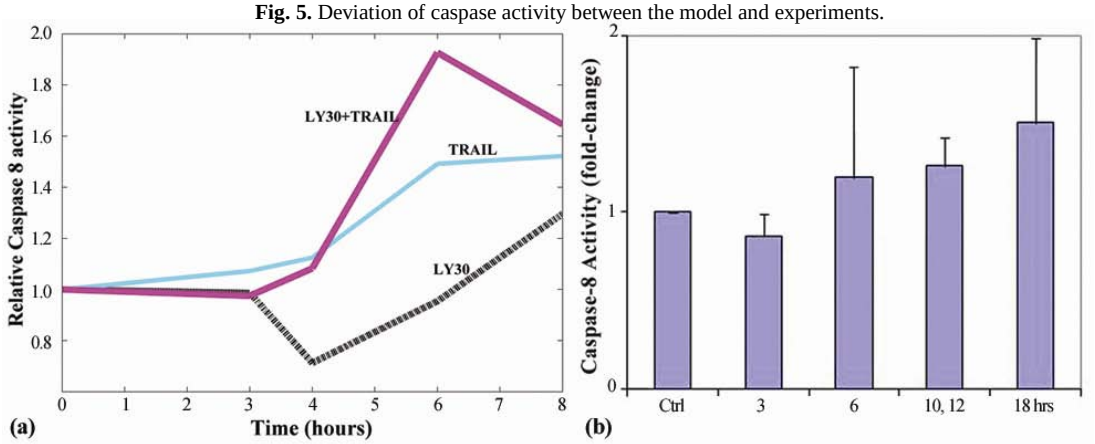

Fig. 6. (a) Experimentally observed caspase-8 activity after treatment with LY30 and/or TRAIL. Single replicate. (b) Caspase-8 activity after LY30 treatment, shown for time points at which 3 or more replicates are available.

levels at 3hrs and 4hrs (6 independent data points) were on average 84% as high as the untreated activation levels, with a p-value < 0.05. Activity levels for caspase-3 and caspase-9 showed similar trends (not shown) but lower statistical significance.

To detect a divergence between our modeling and our data, immediate inspection was sufficient and mathematical modeling was not necessary. Some unknown effect of LY30 must occur, and we could infer it to be upstream of caspase-8 and prior to 3 hours. Knowing that LY30 affects cFLIP, and knowing that cFLIP has complex regulation[35-37], we repeated the measurements of cFLIP including early time-points after treatment with LY30. We found that cFLIP levels, relative to untreated control, increased 30 minutes after LY30 treatment, and declined after one hour, (Fig.7 and Supplement). The early up-regulation is a novel finding, and the late down-regulation agrees with the previous findings by Poh *et al*. Determining fully the mechanisms of cFLIP regulation is beyond the scope of our current work, but it is an important avenue for future research.

Previous studies revealed that Resveratrol, another pro-apoptotic compound that induces intracellular reactive oxygen species, has pro-survival or pro-apoptotic effects depending on the concentration used. Intrigued by this work, we measured cell viability at a series of time points, after treatment with varying dilutions of LY30 (Fig.8). Although we did detect some increased and decreased levels of death depending on concentration, these were not statistically significant.

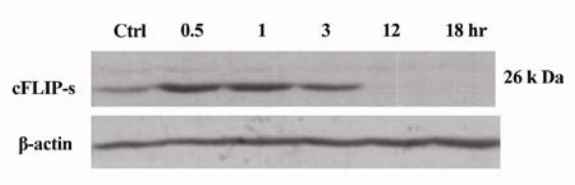

Fig. 7. Western blot analysis of cFLIP-s in Hela after different durations of LY30 treatment.

6. REVISED MODEL

We constructed a revised model of the effects of LY30 on TRAIL-induced apoptosis, but this time instead of using differential equations to govern the production and consumption of cFLIP, we used our immunoblot measurements of cFLIP levels over time (relative to treated) as a time-dependent input[34]. cFLIP data points were interpolated into a continuous curve using linear interpolation in matlab. No other modifications were made. Simulation of this revised model (Fig.9) shows that the synergy between LY30 and TRAIL is now delayed relative to the previous, "naïve" model. This change improves the agreement between simulation and data. The magnitude of this effect and the amount of the delay depends on competition between effects that are poorly calibrated, and requires further study. Likewise, the downstream effects of LY30 and the combination of caspase signaling with other death signals will require further study.

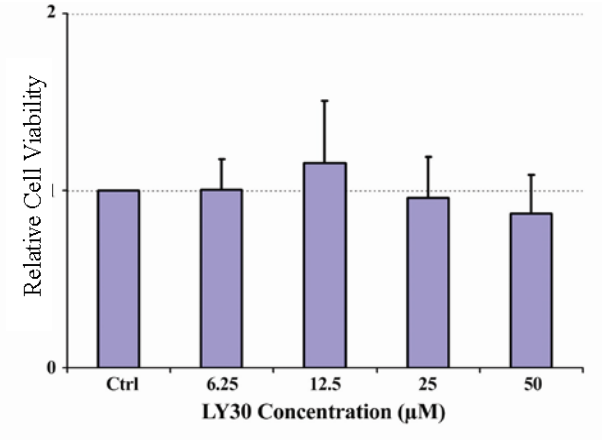

Fig. 8. Relative cell viability after 3 hours of treatment with different concentrations of LY30, based on at least 4 replicates for each dose.

7. DISCUSSION AND CONCLUSION

We constructed an *in silico* model of the effects of LY30 on TRAIL-induced apoptosis. We then detected mismatch between this model and caspase activation data, which led us to experiments showing the existence of a novel and paradoxical caspase inhibitory effect of the drug. This work shows the usefulness of modeling as a guide for identifying unanticipated effects. Namely, we used modeling to represent all known reactions involving a drug, used simulation of the model to infer the indirect effects on the system, and finally compared the simulation against experimental observations of the system, with and without drug treatment, to seek drug-induced phenomena (or lack thereof) that the model did not explain. Previous studies have used kinetic models of signaling pathways to detect that experimentally observed phenomena were lacking from previously accepted pathway models[19,39]. This work is among very few that use pathway modeling to guide experiments towards actually confirming a previously unknown phenomenon[40]. Specifically, we identified that

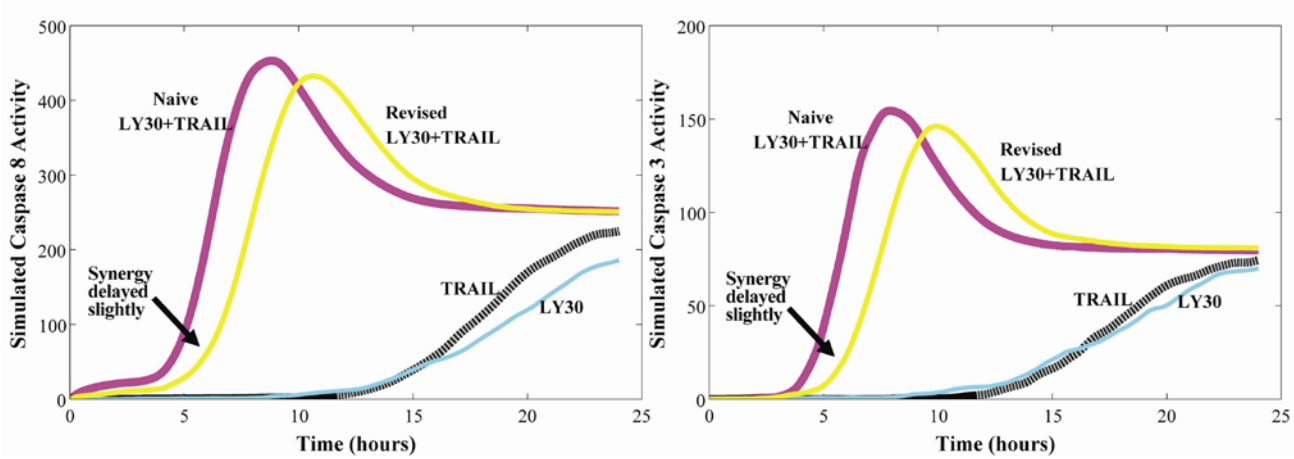

Fig. 9. Simulations (with Monte Carlo sampling) of caspase activation after LY30 and/or TRAIL. Note that revising the model of how LY30 affects cFLIP has no effect on the simulation of LY30 alone nor TRAIL alone. Similar areas under the curve (implying similar cumulative death effects) are observed for the naïve and revised models.

temporary apoptosis-inhibitory effects occur at the level of caspase-8 and cFLIP-s regulation after treatment with LY30. Although cFLIP has complex and potentially contradictory roles in regulating caspase-8 activation[36], the early up-regulation and late down regulation of cFLIP-s is a likely cause for the early inhibition and late stimulation of caspase-8 activation.

Our preliminary identification of this effect is a step towards finding its mechanism and mediators. If H_2O_2 is a key mediator, then this paradoxical early effect may conceivably occur after treatment with a variety of other anti-cancer compounds that also induce H_2O_2[41]. There are also anti-cancer compounds that act by blocking the ATP-binding pockets of one or more kinases (and many kinase inhibitors have overlapping specificities). To the extent that LY30 sensitization effects can be explained by its inhibition of kinases, our results about LY30 may have relevance for understanding the function and for designing chemical optimizations of other kinase inhibitors.

Because the net effect of LY30 is a strong sensitization to TRAIL-induced apoptosis, and because we have evidence for a brief phase when caspase activity is inhibited, one might infer that the later and/or downstream effects of LY30 are even more strongly pro-apoptotic and more potent than previously expected. The up- and down-regulation of cFLIP might alone be sufficient to explain the swing between the early/upstream and late/ultimate effects of LY30. However, we are intrigued by the possibility that other unexplored effects of LY30 may be taking effect, and in future work, we will attempt to use the onset of synergy as a trackable quantum of information along the pathway, to identify other times or reactions with unexplained perturbations by LY30.

Regarding the pharmaceutical implications for LY30, we do not know whether a TRAIL-sensitizing compound with some caspase-inhibitory effects along with strong pro-apoptotic effects would be better or worse than a more specific drug. Even if we knew that LY30 were stimulating multiple competing pathways, we still would not know whether having competing effects would be worse (with decreased apoptotic effect on cancerous cells) or better (with decreased death for normal cells) than a drug with pro-apoptotic effects alone. If the direct targets are identified, this question would be an interesting problem to address using computational modeling. Additional factors that determine the success of a combination therapy arise from considering the effects of the combination on a population of independently evolving cells. For example, a recent study about the evolution of resistance found that antagonistic drug combinations can sometimes have paradoxical benefits, delaying the development of resistance by reducing the selective advantage of cells in a population that have acquired partial resistance[1]. In any case, the effects of LY30 should be investigated experimentally to better understand it and its related compounds, while bearing in mind that short-term caspase inhibitory effects might not have any ultimate effect on long-term cell fate.

In many modeling projects, the direct reactions of a ligand or drug (e.g., the inhibition of particular enzymes, or the activation of particular receptors) are presumed to be known inputs[2]. Assuming a direct reaction to be the sole effect of a drug is risky because even an optimized

inhibitor of a well-studied target may have unanticipated molecular interactions and off-target effects. Therefore our approach of using modeling to study unanticipated effects is potentially relevant for any drug or perturbation, provided it is acting on a well-studied pathway with an existing mathematical model.

The terminology of "match" and "mismatch" may connote to some readers a greater confidence margin than is realistic. A match between model and data does not provide much reassurance, by itself, that the model is correct. Instead a resemblance between model and data should be interpreted as conveying some probabilistic information that the model is more likely to be correct than if it did not match. Conversely, detecting that a model disagrees with experiments, starting at some point (in time or in the network), is not a guarantee that novel biological effects exist at that point. Rather, the model provides clues about what points are more likely than others to contain unknown phenomena. Mismatch analysis may serve as a guide for sampling the space of possible experiments, but it does not provide a firm constraint for a discrete search process. Future research in this area would be aided by the development of more principled statistical methods for comparing qualitative models against unscaled (relative) data.

Simple logic can be used to infer some of the effects of a perturbation on a system, such as inferring that cFLIP down-regulation might have pro-apoptotic effects. With a bit of thought, one can also infer that the effects of LY30[10,11] would be synergistic with TRAIL rather than additive. Human reasoning, however, is not well-suited for estimating the speed and magnitude of competing effects propagating through the network. Computational modeling can serve as a vital tool for data analysis, similar to many other scientific disciplines where the comparison between theory and observation is aided by mathematical methods for extracting complex meaning from experimental data. Computational modeling and experimental investigation, when integrated together, are proving to be a synergistic combination.

8. MATERIALS AND METHODS

8.1. Cell and treatments

HeLa, was purchased from ATCC (Rockville, MD, USA) and maintained in DME supplemented with 10% FBS, 1% L-glutamine, and 1% S-penicillin. HeLa cells were typically plated at 10^5 cells/well in 24-well plates. All treatments with LY30 and TRAIL used the methods and doses of [35]. For example, cells treated with both LY30 and TRAIL were pre-incubated for 1 hr with 25μM of LY30 (Calbiochem, Darmstadt, Germany and Alexis, Switzerland) and then treated with 20 ng/ml of TRAIL (Biomol, Plymouth Meeting, PA, USA) for up to 24 hrs.

8.2. Viability

HeLa cells, after incubation with treatments, were first washed with 1xPBS gently, then stained with crystal violet solution(0.25mL) for 20 minutes. Excess crystal violet solution was washed away three times with distilled water. The remaining crystal violet was then dissolved in 1%SDS with 1XPBS. Thereafter absorbance was measured at 595nm.

8.3. Caspase activity

HeLa cells, after incubation with treatments, were harvested, washed with 1xPBS, re-suspended in chilled cell lysis buffer (BD Pharmingen, San Diego, CA, USA), and incubated on ice for 10 min. Caspase-3 and Caspase-8 enzyme activities were assayed using 7-amino trifluoromethylcoumarin and 7-amino-4-methycoumarin-conjugated substrates (BioMol, Plymouth Meeting, PA, USA) as reported previously [35].

8.4. SDS-PAGE and western blotting

Hela cells were plated (2 x 10^6) in a 60mm Petri dish and treated with the LY30 for the indicated durations. Cells were harvested and washed once with 1X PBS before lysis using cell lysis buffer (150mM Nacl, Tris-Hcl 7.4 and 1% Nonidet P40). Total protein content of the lysates were estimated using the Better Bradford reagent protein estimation kit (Pierce Biotechnology, Rockford, IL, USA). 100μg of cell lysate was then subjected to SDS-PAGE on a 10% polyacrylamide gel before being electro-transferred onto (0.45μ, PVDF) Immobilon-P membranes (Millipore Corporation, Bedford, MA). Membranes were blocked using 5% non-fat dry milk in PBST (PBS with 0.5% tween 20) and probed overnight at 4^{o}C with FLIP antibody (Santa Cruz Biotechnology Inc. Santa Cruz, CA. USA). Anti β-actin (Sigma-Aldrich. St Louis, MO, USA) was used as a loading control. Primary antibodies were detected using

HRP conjugated anti-mouse or anti-rabbit antibodies and visualized using enhanced chemiluminescence detection (ECL reagents from Roche, Indianapolis, IN, USA). Densities were measured using Image J (http://rsb.info.nih.gov/ij/)

8.5. Simulations and Statistics

All events and influences were modeled as elementary reactions with mass action kinetics, and simulated with ordinary differential equations (ODEs). Matlab (Natick, MA, USA) with the KroneckerBio toolbox was used for most simulations[42]. Copasi was used for concept development[30], and CellDesigner for visualization[43]. Synthesis and degradation were limited to caspases, as in [44]. Degradation processes were established using a single rate for all procaspases and a single rate for all activated caspases[44]. Synthesis rates were assigned for each species so that the initial concentrations of the Albeck model would be equal to the steady state of our system without TRAIL. Monte Carlo simulations used 10,000 replications on cells normally distributed about a mean initial concentration vector. Variance levels for the sampling were tested in 10% increments up to 50%, and 40% was chosen because it gave best agreement with data.

All p-values were computed using the one sample t-test with two-tailed distribution using GraphPad (www.graphpad.com)

Author Contributions

Computational modeling was performed by Shi and Tucker-Kellogg. Biological experiments were performed by Shi, Huang, and Varghese. Data analysis and figures were done by Tucker-Kellogg, Shi, and Varghese. Supervision was provided by Tucker-Kellogg, White, and Pervaiz. Project was designed by Tucker-Kellogg. Text was written by Tucker-Kellogg and edited by all authors.

Acknowledgments

We gratefully acknowledge assistance from Jared Toettcher, Kwok-Gwee Siew Ing, Andrea Holme, and Kothandharaman Subramaniam. This work was supported by a fellowship and grant from the Lee Kuan Yew Foundation to Tucker-Kellogg, by NUS "cross-faculty grant" R-252-000-351-123 to Tucker-Kellogg & Pervaiz, and by Singapore-MIT Alliance grants C-382-641-004-091 to White and Tucker-Kellogg and C-382-641-001-091 to Pervaiz.

References

1. Chait R, Craney A, Kishony R. Antibiotic interactions that select against resistance. *Nature*. 2007; **446**: 668-671.
2. Fitzgerald JB, Birgit S, Nielsen UB, Peter KS. Systems biology and combination therapy in the quest for clinical efficacy. *Nature Chem Bio*. 2006; **2**: 458-466.
3. Kwang HL, Jin HP, Tae YK, Hyun UK, Sang YL. Systems metabolic engineering of Escherichia coli for L-threonine production. *Molecular Systems Biology* 2007; **3**:149.
4. Falschlehner C, Emmerich CH, Gerlach B, Walczak H. TRAIL signaling: Decisions between life and death. *Int J Biochem Cell Biol*. 2007; **39**: 1462-1475.
5. Bouralexis S, Findlay DM, Evdokiou A. Death to the bad guys: Targeting cancer via Apo2L/TRAIL. *Apoptosis*. 2005; **10**: 35-51.
6. L Zhang, B Fang. Mechanisms of resistance to TRAIL-induced apoptosis in cancer. *Cancer Gene Therapy* 2005; **12**: 228–237.
7. Lee JY, Huerta YS, Vega M, Baritaki S, Spandidos DA, Bonavida B. The NO TRAIL to YES TRAIL in cancer therapy. *Int J Oncol*. 2007; **4**: 685-691.
8. Walker EH, Pacold ME, Perisic O, Stephens L, Williams RL *et al*. Structural determinants of phosphoinositide 3-kinase inhibition by wortmannin, LY294002, quercetin, myricetin, and staurosporine. *Mol Cell*. 2000; **6**: 909-919.
9. Wang S. The promise of cancer therapeutics targeting the TNF-related apoptosis-inducing ligand and TRAIL receptor pathway. *Oncogene*. 2008; **27**: 6207-6215.
10. Poh TW, Pervaiz S. LY294002 and LY303511 sensitize tumor cells to drug-induced apoptosis via intracellular hydrogen peroxide production independent of the phosphoinositide 3-kinase-Akt pathway. *Cancer Res*. 2005; **65**: 6264-6274.
11. Shenoy K, Wu Y, Pervaiz S. LY303511 enhances TRAIL sensitivity of SHEP-1 neuroblastoma cells via hydrogen peroxide-mediated mitogen-activated protein kinase activation and up-regulation of death receptors. *Cancer Res*. 2009; **69**: 1941-1950.
12. Davies SP, Reddy H , Caivano M, Cohen P . Specificity and mechanism of action of some commonly used protein kinase inhibitors. *Biochem. J.* 2000; **351**: 95-105.

13. Jacobs MD, Black J, Futer O, Swenson L, Hare B, *et al*. Pim-1 ligand-bound structures reveal the mechanism of serine/threonine kinase inhibition by LY294002. *J Biol Chem*. 2005; **280**: 13728-13734.
14. Kristof AS, Pacheco RG, Schremmer B, Moss J. LY303511 (2-piperazinyl-8-phenyl-4H-1-benzopyran-4-one) acts via phosphatidylinositol 3-kinase-independent pathways to inhibit cell proliferation via mammalian target of rapamycin (mTOR)- and non-mTOR-dependent mechanisms. *J Pharmacol Exp Ther*. 2005; **314**: 1134-1143.
15. Gharbi SI, Zvelebil MJ, Shuttleworth SJ, Hancox T, Waterfield MD, *et al*. Exploring the specificity of the PI3K family inhibitor LY294002. *Biochem J*. 2007; **404**: 15-21.
16. Albeck JG, Burke JM, Aldridge BB, Zhang M, Lauffenburger DA, Sorger PK. Quantitative analysis of pathways controlling extrinsic apoptosis in single cells. *Mol Cell*. 2008; **30**: 11-25.
17. Albeck JG, Burke JM, Spencer SL, Lauffenburger DA, Sorger PK. Modeling a snap-action, variable-delay switch controlling extrinsic cell death. *PLoS Biol*. 2008; **6**: 2831-2852.
18. Bagci EZ, Vodovotz Y, Billiar TR, Ermentrout GB, Bahar I. Bistability in apoptosis: roles of bax, bcl-2, and mitochondrial permeability transition pores. *Biophys J*. 2006; **90**: 1546-1559.
19. Eissing T, Conzelmann H, Gilles ED, Allgöwer F, Bullinger E, Scheurich P. Bistability analyses of a caspase activation model for receptor-induced apoptosis. *J Biol Chem*. 2004; **279**: 36892-36897.
20. Hua Z, Ruomei Y, Junshan H, Jean Wg, Robert CA, *et al*. Regulation of the Apaf-1/Caspase-9 Apoptosome by Caspase-3 and XIAP. *J. Biol. Chem*. 2003; **278**: 8091-8098.
21. Kruez S, Siegmund D, Scheurich P, Wajant H. NF-kB inducers upregulate cFLIP, a cycloheximide-sensitive inhibitor of death receptor signaling. *Molecular and cellular biology*. 2001; **21**: 3964–3973.
22. Nitobe J, Yamaguchi S, Okuyama M, Nozaki N, Sata M *et al*. Reactive oxygen species regulate FLICE inhibitory protein (FLIP) and susceptibility to Fas-mediated apoptosis in cardiac myocytes. *Cardiovasc Res*. 2003; **57**: 119-128.
23. Ahmad KA, Iskandar KB, Hirpara JL, Clement MV, Pervaiz S. Hydrogen peroxide-mediated cytosolic acidification is a signal for mitochondrial translocation of Bax during drug-induced apoptosis of tumor cells. *Cancer Res*. 2004; **64**: 7867-7878.
24. Clément MV, Pervaiz S. Intracellular superoxide and hydrogen peroxide concentrations: a critical balance that determines survival or death. *Redox Rep*. 2001; **6**: 211-214.
25. Hirpara JL, Clément MV, Pervaiz S. Intracellular acidification triggered by mitochondrial derived hydrogen peroxide is an effector mechanism for drug induced apoptosis in tumor cells. *J Biol Chem*. 2001; **76**: 514-521.
26. Pervaiz, S, Clément MV. Hydrogen peroxide-induced apoptosis: oxidative or reductive stress? *Methods Enzymol*. 2002; **352**: 150-159.
27. Yamakawa H, Ito Y, Naganawa T, Banno Y, Nakashima S, Sakai N *et al*. Activation of caspase-9 and -3 during H2O2-induced apoptosis of PC12 cells independent of ceramide formation. *Neurol Res*. 2000; **22**: 556-564.
28. Zuo Y, Xiang B, Yang J, Sun X, Yi J *et al*. Oxidative modification of caspase-9 facilitates its activation via disulfide-mediated interaction with Apaf-1. *Cell Res*. 2009; **19**: 449-457.
29. H Choi, Han S, Yokota H, Cho KH. Coupled positive feedbacks provoke slow induction plus fast switching in apoptosis. *FEBS Letters*. 2007; **581**: 2684-2690.
30. Hoops S, Sahle S, Gauges R, Lee C, Pahle J, *et al*. COPASI--a COmplex PAthway SImulator. *Bioinformatics*. 2006; **22**: 3067-3074.
31. Koh G, Teong HC, Clément MV, David Hsu, Thiagarajan PS. A decompositional approach to parameter estimation in pathway modeling: a case study of the Akt and MAPK pathways and their crosstalk. *ISMB* (Supplement of Bioinformatics) 2006; 271-280.
32. Koh G, Tucker-Kellogg L, Hsu D, Thiagarajan PS. Globally consistent pathway parameter estimates through belief propagation. Proceedings of 7th *Workshop on Algorithms in Bioinformatics* (WABI) September 2007; 420-430.
33. Moles CG, Mendes P, Banga JR. Parameter estimation in biochemical pathways: a comparison of global optimization methods. *Genome Res*. 2003; **13**: 2467-2474.
34. Van Riel NA, Sontag ED. Parameter estimation in models combining signal transduction and metabolic pathways: The dependent input approach. *Syst Biol*. 2006; **153**: 263-274.
35. Poh TW, Huang S, Hirpara JL, Pervaiz S. LY303511 amplifies TRAIL-induced apoptosis in tumor cells by enhancing DR5 oligomerization, DISC assembly, and mitochondrial permeabilization. *Cell Death Differ*. 2007; **14**: 1813-1825.

36. Peter ME. The flip side of FLIP. *Biochem J*. 2004; **382**: e1-3.
37. Fukazawa T, Fujiwara T, Uno F, Teraishi F, Tanaka N, *et al*. Accelerated degradation of cellular FLIP protein through the ubiquitin-proteasome pathway in p53-mediated apoptosis of human cancer cells. *Oncogene* 2001; **20**: 5225-5231
38. Wajantdagger H, Haasdagger E, Schwenzerdagger R, Mühlenbeckdagger F, Scheurichdagger P *et al*. Inhibition of death receptor-mediated gene induction by a cycloheximide-sensitive factor occurs at the Level of or upstream of Fas-associated Death Domain Protein (FADD). *J. Biol. Chem*. 2000; **275**: 24357-24366.
39. Smieja J, Jamaluddin M, Brasier AR and Kimmel M. Model-based analysis of interferon-beta induced signaling pathway. *Bioinformatics*. 2008; **24**: 2363-2369.
40. Hua F, Cornejo MG, Cardone MH, Stokes CL, Lauffenburger DA. Effects of Bcl-2 levels on Fas signaling-induced caspase-3 activation: molecular genetic tests of computational model predictions. J *Immunol*. 2005; **175**: 985-995.
41. Mizutani H, Tada OS, Hiraku Y, Kojima M, Kawanishi S. Mechanism of apoptosis induced by doxorubicin through the generation of hydrogen peroxide. *Life Sci*. 2005; **76**: 1439-1453.
42. Apgar JF, Toettcher JE, White JK and Tidor B. Unpublished.
43. Funahashi, A, Matsuoka, Y, Jouraku A, Morohashi M, Kikuchi N, Kitano H. CellDesigner 3.5: A Versatile Modeling Tool for Biochemical Networks; Proceedings of the *IEEE*. 2008; **96**: 1254-1265.
44. Bentele M, Lavrik I, Ulrich M, Stösser S, Heermann DW, *et al*. Mathematical modeling reveals threshold mechanism in CD95-induced apoptosis. *J Cell Biol*. 2004; **166**: 839-851.

APPENDIX A

REACTION EQUATIONS FOR MODELING APOPTOSIS INDUCED BY TRAIL AND LY30.

Molecule names are abbrevated as in [16-17]. For example, procaspase-8 is called C8 and caspase-8 is C8*, with asterisks indicating active forms of a protein.

$$TRAIL + R \underset{k\_1}{\overset{k1}{\rightleftarrows}} TRAIL:R \xrightarrow{KK1} R^*$$

$$R^* + flip \underset{k\_2}{\overset{k2}{\rightleftarrows}} R^*:flip$$

$$R^* + C8 \underset{k\_3}{\overset{k3}{\rightleftarrows}} R^*\ C8 \xrightarrow{KK3} R^* + C8^*$$

$$C8^* + BAR \underset{k\_4}{\overset{k4}{\rightleftarrows}} C8^*:BAR$$

$$C8^* + C3 \underset{k\_5}{\overset{k5}{\rightleftarrows}} C8^*:C3 \xrightarrow{KK5} C8 + C3^*$$

$$C3^* + C6 \underset{k\_6}{\overset{k6}{\rightleftarrows}} C3^*:C6 \xrightarrow{KK6} C3^* + C6^*$$

$$C6^* + C8 \underset{k\_7}{\overset{k7}{\rightleftarrows}} C6^*:C8 \xrightarrow{KK7} C6^* + C8^*$$

$$C3^* + XIAP \underset{k\_8}{\overset{k8}{\rightleftarrows}} C3^*:\ XIAP \xrightarrow{KK8} XIAP$$

$$C3^* + PARP \underset{k9}{\overset{k9}{\rightleftarrows}} C3^*:PARP \xrightarrow{KK9} C3^* + cPARP$$

$$C8^* + Bid \underset{k\_10}{\overset{k10}{\rightleftarrows}} C8^*:Bid \xrightarrow{KK10} C8^* + tBid$$

$$tBid + Bcl2c \underset{k\_11}{\overset{k11}{\rightleftarrows}} tBid:Bcl2c$$

$$tBid + Bax \underset{k\_12}{\overset{k12}{\rightleftarrows}} tBid:Bax \xrightarrow{KK12} tBid + Bax^*$$

$$Bax^* \underset{k\_13}{\overset{k13}{\rightleftarrows}} Baxm^*$$

$$Baxm^* + Bcl2 \underset{k\_14}{\overset{k14}{\rightleftarrows}} Baxm^*:Bcl2$$

$$Baxm^* + Baxm^* \underset{k\_15}{\overset{k15}{\rightleftarrows}} Bax2$$

$$Bax2 + Bcl2 \underset{k\_16}{\overset{k16}{\rightleftarrows}} Bax2:Bcl2$$

$$Bax2 + Bax2 \underset{k\_17}{\overset{k17}{\rightleftarrows}} Bax4$$

$$Bax4 + Bcl2 \underset{k\_18}{\overset{k18}{\rightleftarrows}} Bax4:Bcl2$$

$$Bax4 + M \underset{k\_19}{\overset{k19}{\rightleftarrows}} Bax4:M \xrightarrow{KK19} M^*$$

$$M^* + Cycm \underset{k\_20}{\overset{k20}{\rightleftarrows}} M^*:Cycm \xrightarrow{KK20} M^* + Cycr$$

$$M^* + Smacm \underset{k\_21}{\overset{k21}{\rightleftarrows}} M^*:Smacm \xrightarrow{KK21} M^* + Smacr$$

$$Cycr \underset{k\_22}{\overset{k22}{\rightleftarrows}} Cyc$$

$$Cyc + Apaf \underset{k\_23}{\overset{k23}{\rightleftarrows}} Cyc:Apaf \xrightarrow{KK23} Cyc + Apaf^*$$

$$Apaf^* + C9 \underset{k\_24}{\overset{k24}{\rightleftarrows}} Apop$$

$$Apop + C3 \underset{k\_25}{\overset{k25}{\rightleftarrows}} Apop:C3 \xrightarrow{KK25} Apop + C3^*$$

$$Smacr \underset{k\_26}{\overset{k26}{\rightleftarrows}} Smac$$

$$Apop + XIAP \underset{k\_27}{\overset{k27}{\rightleftarrows}} Apop:XIAP$$

$$XIAP + Smac \underset{k\_28}{\overset{k28}{\rightleftarrows}} Smac:XIAP$$

$$C8^* \xrightarrow{KK29} \phi$$

$$C3^* \xrightarrow{KK29} \phi$$

$$C6^* \xrightarrow{KK29} \phi$$

$$Apop \xrightarrow{KK29} \phi$$

$$C8 \xrightarrow{KK30} \phi$$

$$C3 \xrightarrow{KK30} \phi$$

$$C6 \xrightarrow{KK30} \phi$$

$$C9 \xrightarrow{KK30} \phi$$

$$\phi \xrightarrow{KK31} C8$$

$$\phi \xrightarrow{KK32} C6$$

$$\phi \xrightarrow{KK33} C3$$

$$\phi \xrightarrow{KK34} C3$$

$$LY30 \xrightarrow{k35} LY30 + ROS$$

$$ROS + pro\_apop \xrightarrow{k36} Apoptosis$$

$$ROS + C9 \underset{k\_37}{\overset{k37}{\rightleftarrows}} ROS:C9 \xrightarrow{KK37} ROS + Apop$$

$$ROS \xrightarrow{k38} \phi$$

$$LY30 + R \underset{k\_39}{\overset{k39}{\rightleftarrows}} LY30:R \xrightarrow{KK39} LY30 + R\_oligo$$

$$TRAIL + R\_oligo \underset{k\_40}{\overset{k40}{\rightleftarrows}} TRAIL:R\_oligo \xrightarrow{KK40} R^*$$

$$LY30 + flip \xrightarrow{k41} LY30$$

$$LY30 \xrightarrow{k42} \phi$$

$$C3^* + C9 \underset{k\_43}{\overset{k43}{\rightleftarrows}} C3^*:C9 \xrightarrow{KK43} Apop + C3^*$$